Hindawi
International Journal of Photoenergy
Volume 2019, Article ID 3057929, 16 pages
https://doi.org/10.1155/2019/3057929

Review Article

Recent Advances on Renewable and Biodegradable Cellulose Nanopaper Substrates for Transparent Light-Harvesting Devices: Interaction with Humid Environment

Alessandra Operamolla

Dipartimento di Chimica, Università degli Studi di Bari Aldo Moro, Via Orabona 4, I-70126 Bari, Italy

Correspondence should be addressed to Alessandra Operamolla; alessandra.operamolla@uniba.it

Received 21 September 2018; Revised 26 March 2019; Accepted 9 May 2019; Published 10 June 2019

Academic Editor: Giulia Grancini

Cellulose nanopaper (CNP) has attracted much interest during the last decade as a new fascinating renewable and biodegradable substrate for printed electronics and solar cells. Its outstanding optical and mechanical properties make CNP the ideal substrate for the preparation of photovoltaic devices, since its high transparency and haze favour the absorption of light from the active layer of the solar cell. However, some advances need to be done in the direction of increasing CNP stability in humid environment without compromising its remarkable advantages. This review critically points at these aspects, presenting an overview of state-of-art solutions to enhance nanopaper stability in a humid environment.

1. Introduction

The compelling need for alternative and renewable energies is, nowadays, meeting the necessity to produce cheap and affordable devices, able to convert light into electrical energy, while being benign for the environment. For this reason, considerable efforts must be put in the direction of enabling reliable, efficient, and cheap smart devices deposited on biodegradable and renewable biomaterials. With this respect, cellulose represents the ideal candidate: it is a well-known, abundant, cheap, and affordable biomaterial derived from plants, whose existence is known to us from 1838 [1]. Cellulose technological importance is linked to papermaking industry and to the preparation of other cellulose products, like rayon and cellophane, that are part of our life for decades. In parallel, new challenges have arisen, connected to industrial and academic research on the conversion of cellulose into biofuels or into other high-value products [2].

In particular, paper industry, with a world production of ~420 billion of kg per year [3], would receive a very fruitful payback from the integration of cellulose paper into the market of printed electronics. This market will worth over 73 billion dollars by 2027 [4]. Moreover, a number of printing technologies for paper are already available [5]. The economic convenience is sided by other not-secondary advantages: the biodegradability, allowing the easy recovery of the device active layers after service; the biocompatibility, suggesting the possible integration of a device into patches and other medical aids; and the harmlessness for the environment in case of accidental device release.

Standard paper is opaque and displays a rough surface, with spaces among paper fibres that need to be filled with specific materials, able to improve paper compatibility with electronic inks. For this reason, an extensive research on paper modification is already in progress and the state-of-the-art has been reviewed recently [6]. Yet, even after surface modification, standard paper still lacks the property of transparency that would greatly widen its applications, making it a perfect substrate for devices such as solar cells and light-emitting diodes. This justifies the present efforts to attain transparent paper, with the aim to access cheaper and more sustainable substrates for electronic devices than poly(ethylene terephthalate) (PET) or poly(ethylene naphthalate) (PEN). This could be done by different approaches, including infiltration of transparent material into opaque paper [7–10], cellulose paper swelling

or redissolving followed by pressing, [11] cellulose composites [12], and cellulose nanopaper (CNP) [13].

In particular, cellulose nanopaper has received a high attention during the past decade for its clean manufacture and its outstanding optical, thermal, and mechanical properties [14] and for its compatibility with printing technologies [15]. Its transparency, combined with the above mentioned features, has increased the interest towards cellulose nanopaper, attracting the attention of the scientific and industrial communities, especially as substrate for optoelectronic devices. The smooth surface of CNP offers unique possibilities for the deposition of the device active layers. However, its hydrophilic character poses some challenges mainly pertinent to its shape stability and resistance to humidity. This is an issue that present research is currently facing, and this review aims at giving a state-of-the-art on the chemical approaches that have been adopted so far to improve CNP resistance to humid environment.

2. Cellulose Nanopaper (CNP): Properties and Potentialities as Substrate for Photoconverting Devices

2.1. Properties of Cellulose Nanopaper

2.1.1. Transparency and Haze. A first classification of cellulose nanocrystalline materials can be done according to TAPPI standards: [16] CNFs and CNCs are cellulose fibres featuring a high aspect ratio. CNCs display a diameter ranging from 5 to 50 nm and length between 100 and 500 nm, while cellulose nanofibres (CNFs) are classified as aggregates of elementary fibres with a diameter between 20 and 50 nm and length between 500 and 2000 nm. Though a major difference is given by their dimension, the cellulose nanomaterials present other differences due to their origin, which influences, among other properties, the crystallinity index. An example of both types of nanostructures is shown in Figures 1(a) and 1(b), where microscopies of (a) CNFs from oat straw [17] and (b) CNCs from ramie [18] are presented. These materials can be isolated from cellulose pulp by diverse top-down approaches, applicable at the laboratory or industrial scale, that have been reviewed by other authors [19].

CNP is an architecture composed of cellulose nanofibres (CNFs) or nanocrystals (CNCs). When the nanocelluloses form a self-standing nanopaper film, they interconnect with each other by establishing interfibre hydrogen bonds, yielding a "nanodimensioned network" similar to the one formed by standard paper fibres. The insets of Figure 1(c) show the surface morphology of paper (right) and nanopaper (left) recorded by SEM microscopy: even if the two materials are formed by the association of cellulose fibres, the level of magnification needed to analyse their morphology is strikingly different. The visual comparison between nanopaper and filter paper is outstanding as well [13]. Optical transparency is the macroscopic property, possessed by CNP, that demonstrates the difference existing between the two materials that is relevant to the dimension of the crystalline fibres. Transparency in CNP arises from the reduced interstice dimension between fibres: nanopaper will display a more homogeneous diffraction index minimizing back scattering.

At the same time, transparency is often accompanied by another fundamental property, haze. Haze is defined as the ratio between the light transmitted through nanopaper (deviated from the incident light beam of an angle above 2.5°) and the total transmitted light intensity. A high haze allows light coupling and responses not depending from the angle of incident light [8]. This property is considered particularly beneficial when the active layer of a solar cell is deposited on CNP, since haze can increase the path length of light in the light-harvesting layers [20]. Figure 2(a) shows a schematic representation of CNP structure and what the haze effect consists of.

Fang et al. [20] demonstrated that the forward scattering angle is dependent on the dimension of the nanofibre-composing paper. The haze was measured on nanopaper composites derived from mixing fibres of different dimension. In particular, CNFs were mixed with wood pulp fibres (mm long and μm wide fibres) in different proportions. Figures 2(b)–2(g) show the appearance of CNP films and the scattering angle they produce at 100% (b, e), 50% (c, f), and 0% (d, g) nanofibres content with respect to wood pulp fibres. The lowest scattering angle was attained when the nanopaper was composed of 100% nanofibrillated cellulose.

2.1.2. Thermal Stability. Cellulose shows remarkable thermal stability if compared to plastics, like PET or PEN, and displays a low thermal expansion coefficient (CTE~28-40 ppm K^{-1}) [22]; therefore, it is the ideal substrate for deposition processes in which curing of the active layers is required. In the case of CNP prepared from cellulose nanofibres isolated from wood pulp, the optical transparency was found unaffected by thermal treatments: curing the nanopaper for 60 minutes at temperatures up to 180°C yielded self-standing CNPs with preserved transparency and without any yellowing due to unwanted oxidation. The outstanding results were witnessed by recording unchanged transmittance spectra (Figure 3) [23].

Conversely, if the nanofibres are functionalized by carboxyl groups on their surface, the thermal durability of cellulose may be compromised [24]. TEMPO-mediated oxidation, a method for producing nanofibres, is the chemical treatment that oxidizes the C_6 carbon of the surface glucopyranosidic groups to -COOH functionalities. Thermogravimetric analyses have been performed on nanopaper and have shown a dramatic decrease of thermal stability in nanopaper prepared from carboxylated nanofibres [25]. This may negatively impact the implementation of nanopaper into device technology, because it can limit the application of annealing processes.

Likewise, other functional groups introduced on the surface of nanocelluloses have been considered responsible of a decrease of thermal stability: for instance, a negative influence of the degree of surface sulphatation on the thermal stability of CNCs was demonstrated [26]. These studies are, however, still in their beginning, and no literature evidence has been given yet on the real influence of the way the

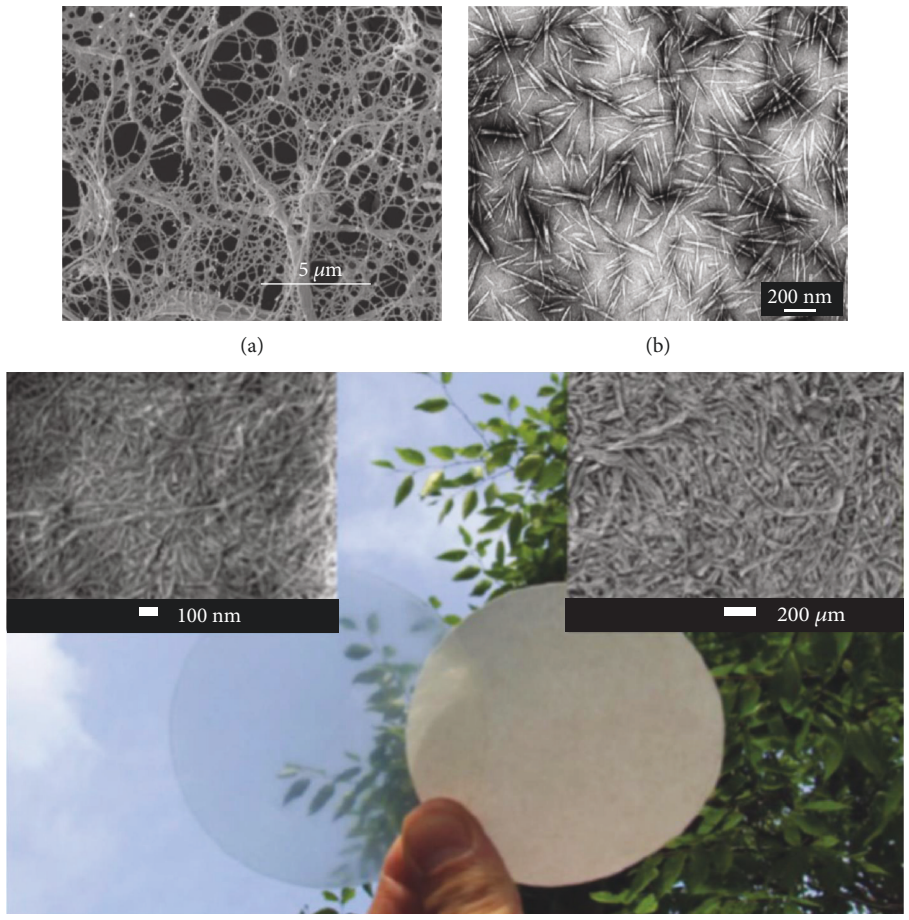

Figure 1: (a) FE-SEM micrograph of cellulose nanofibres (CNFs) obtained by a mechanical disintegration process with a high-pressure homogenizer from oat straw. Scale bar: 5 μm. Reproduced from cellulose, reference [17], with permission from Springer. (b) TEM micrograph of cellulose nanocrystals (CNCs) with 6-8 nm diameter and 150-250 nm length, obtained from purified ramie fibres by H_2SO_4 hydrolysis. Scale bar: 200 nm; reproduced from the Journal of Materials Chemistry, reference [18], with permission from the Royal Society of Chemistry. (c) Nanopaper (left) and filter paper (right) comparison. Optically transparent CNP (left) is composed of 150 nm long CNCs. The upper left inset, with a scale bar of 100 nm, shows a SEM micrograph of the surface of transparent nanopaper. Conventional cellulose paper (right) consists of pulp fibres with 30 μm diameter. The upper right inset, with a scale bar of 200 μm, shows the SEM micrograph of the surface of a sample of filter paper. Reproduced from Advanced Materials, reference [13], with permission from John Wiley and Sons.

nanofibres or nanocrystals are isolated and the true durability of the nanopaper.

2.1.3. Surface Smoothness, Reduced Porosity, and Gas Barrier Properties. CNF and CNC films display exceptional smoothness, a highly desirable property compatible with thin film device deposition. Typically, surface smoothness of cellulose nanopaper is in the range $2 \div 5$ nm, with a porosity of $20 \div 40\%$ and a pore size below 50 nm [14]. The smoothness allows deposition on the nanopaper surface of homogeneous and regular thin films, preventing risk of film cracks and defects and makes the surface of nanopaper compatible with printing techniques. This is particularly important for solution-processed devices, where the smoothness of the substrate is one of the properties influencing the active layer morphology [27]. The high porosity of standard paper is, indeed, one of the most unwanted drawbacks experimented for the deposition of conductive inks: the presence of pores (that in the case of standard paper may reach 3-5 μm dimension) determines excessive material consumption; moreover, due to the high porosity, printed lines may present wavy contours. This leads to a loose of precision of the printing process, which is undesirable for many applications. Hsieh et al. [28] used substrates pulp paper, produced from 50 μm wide fibres and presenting numerous large cavities of around 20–60 μm size, and nanopaper, produced from 30 nm wide nanofibres. They printed 1 mm wide and 40 mm long conductive lines using silver nanoparticle inks on both (Figures 4(a)–4(d)) and found that the conductivity of the printed electrodes was strongly affected by the dimension of the fibres. The smoother and less porous nanopaper allowed to print more efficient conductive lines, presenting comparable performances in terms of conductivity of reference lines printed on polyimide (Figure 4(e)).

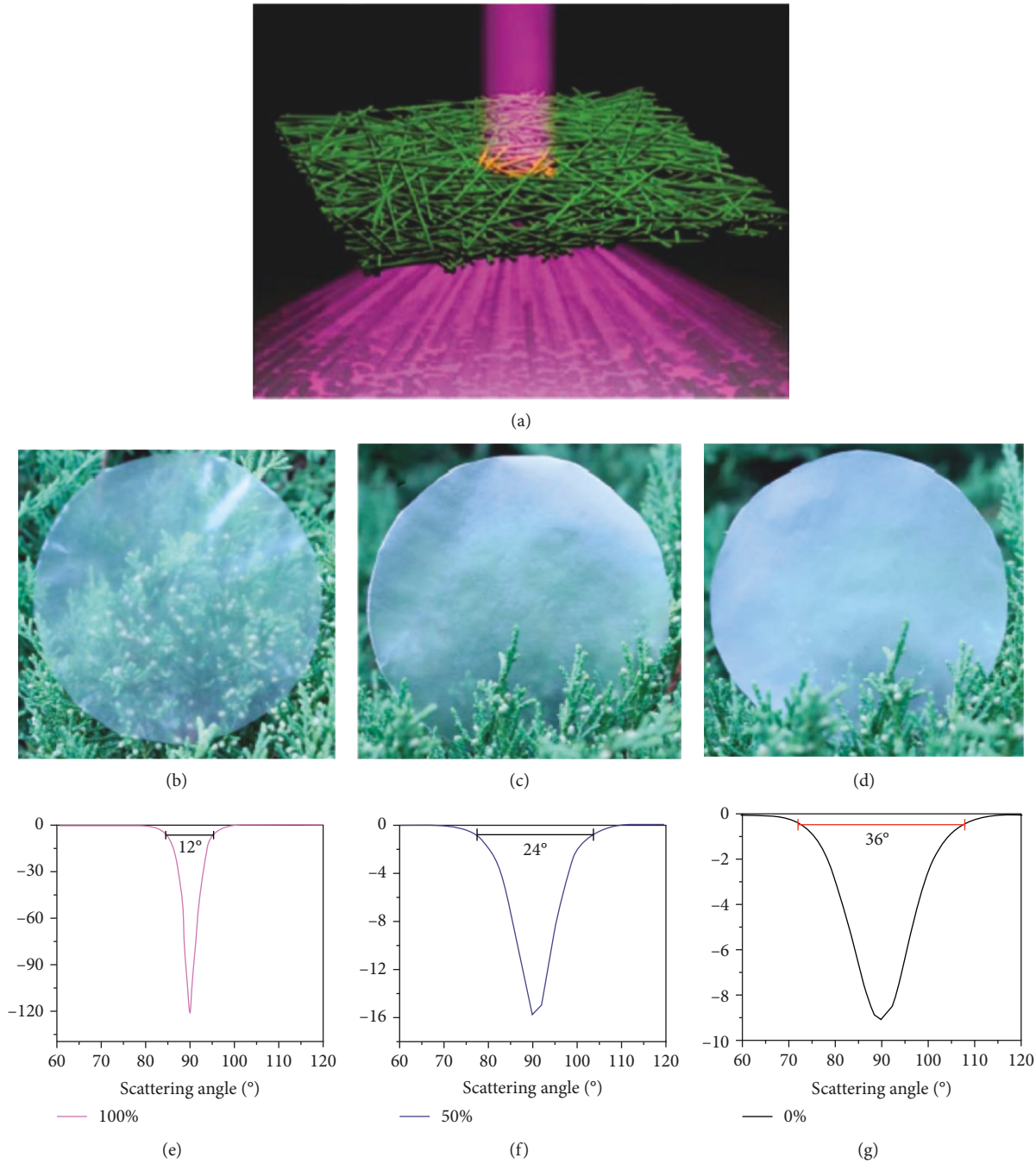

Figure 2: (a) Schematic representation of nanocellulose paper and haze effect. Reproduced from reference [21] with permission from the Royal Society of Chemistry. Visual appearances of the transparent papers with CNF contents of (b) 100%, (c) 50%, and (d) 0%, respectively. Distribution of the scattering angle and maximum scattering angle for the transparent papers (b–d) with a different ratio of CNFs to the whole cellulose content: (e) 100%, (f) 50%, and (g) 0% CNFs. Reproduced from reference [20] with permission from the Royal Society of Chemistry.

Moreover, the continuous film-like structure possessed by CNP endows nanocellulose thin films with good gas barrier properties. It was demonstrated that the oxygen permeability under dry conditions of a polylactic acid (PLA) film was dramatically reduced from 746 mL m^{-2} day^{-1} Pa^{-1} to 1 mL m^{-2} day^{-1} Pa^{-1} after casting of a layer of TOCN (TEMPO-oxidized cellulose nanofibres) on the thin film [29]. This impressive result renders the gas barrier properties of nanocelluloses close to the ones of other synthetic materials, like poly(vinylidene chloride) and polyethyl-ene-poly(vinyl alcohol) copolymers, and is associated with the low porosity of nanocellulose thin films. Later, it was found that the smaller the fibres composing the nanopaper, the higher the gas barrier properties [30].

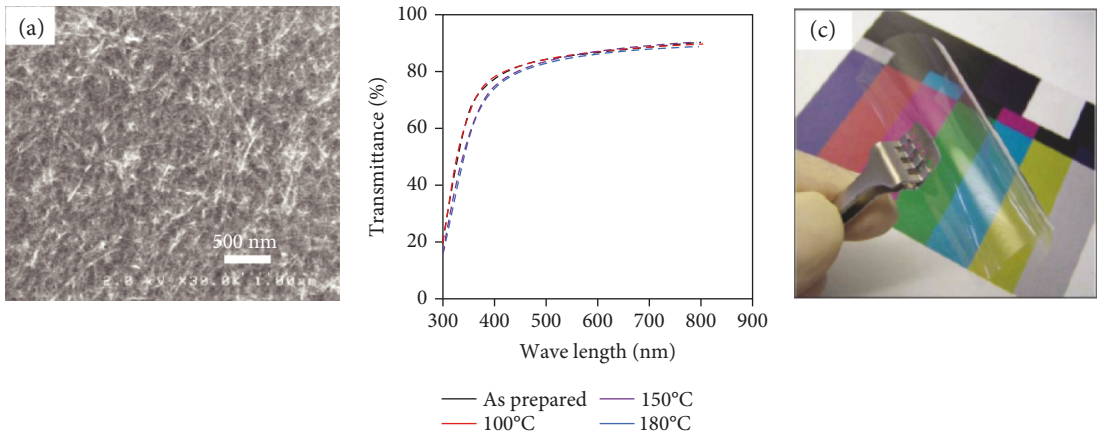

Figure 3: (a) Scanning electron microscopy image of CNF nanopaper. Scale bar: 500 nm. (b) Transmittance spectra of nanopaper: as prepared (black); cured at 100°C (red); cured at 150°C (violet); cured at 180°C (blue). Nanopaper retained excellent light transmittance after curing. (c) Appearance of a 20 μm thick transparent CNP after 180°C curing. Reproduced from reference [23] with permission from John Wiley & Sons.

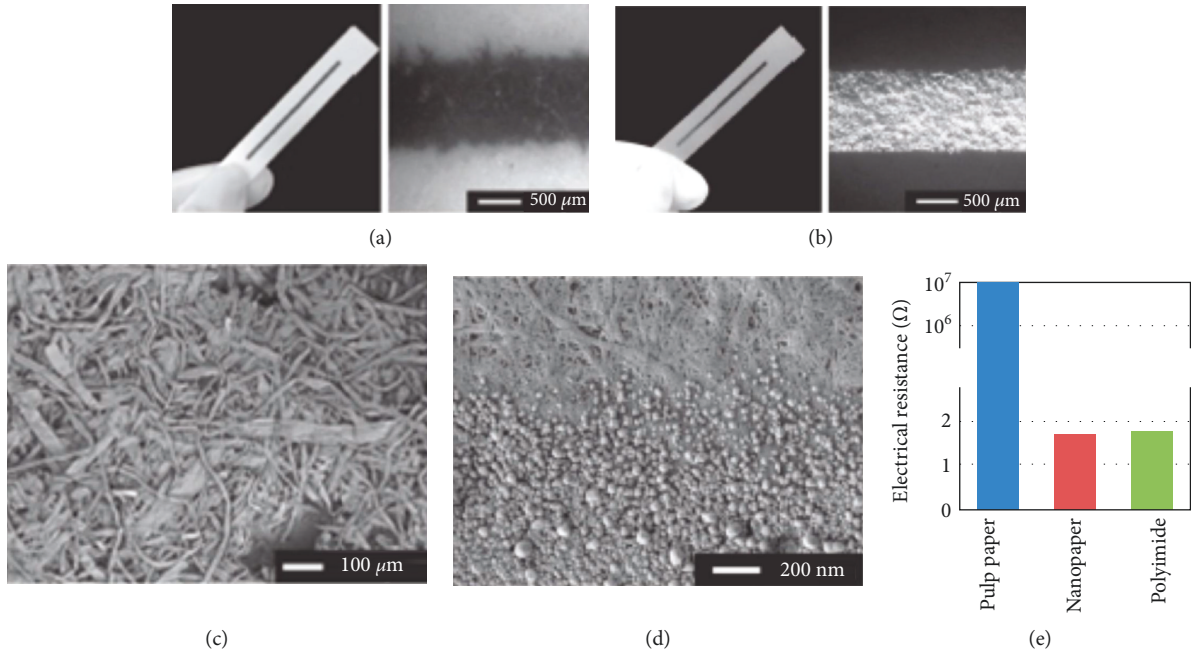

Figure 4: Lines of silver nanoparticles printed on (a) pulp paper and (b) nanopaper. (c, d) SEM micrographs of the printed lines/substrates, with scale bars of 100 μm for pulp paper and 200 nm for nanopaper. (e) Electrical resistance in ohm of the silver nanoparticle lines deposited on pulp paper (blue), nanopaper (red), and control sample on polyimide (green). Reproduced from reference [28] with permission from the Royal Society of Chemistry.

2.1.4. Mechanical Stability. Nanofibril fracture usually controls the mechanical strength of cellulose nanopaper. The stress-strain behavior is connected to the fibre characteristics, and it was demonstrated that average molecular weight possessed by the nanocelluloses used for CNP formation has an influence on their mechanical resistance. Films of nanofibrils differing for the polymerization degree (DP, i.e., the average number of monomeric unit in a single cellulose chain composing the nanocrystals or nanofibres) roughly follow the same stress-strain curve. The chart in Figure 5 shows stress-strain behavior for nanofibril networks prepared from fibres with DP 410 (blue), 580 (green), 820 (red), and 1100 (black). The line break corresponds to strain-to-failure, i.e., the maximum percentage elongation sustained by the films. It is clear from the graph that the highest DP corresponds to the highest strain-to-failure [31]. However, failure is suggested to occur by slippage of the extended cellulose chains rather than by covalent bond breakage.

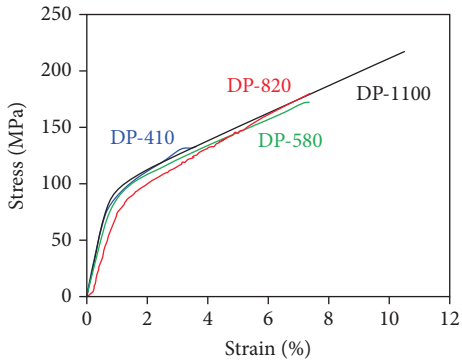

Figure 5: Typical stress-strain curves in uniaxial tension for cellulose nanofibril networks prepared from nanocelluloses with different degrees of polymerization (DP). DP = 410 (blue); DP = 580 (green); DP = 820 (red); DP = 1100 (black) solid lines. Reproduced from reference [31] with permission from the American Chemical Society.

2.1.5. Environmental Compatibility. The biodegradability of cellulose nanopaper is settled. Microorganisms (moulds, fungi, and bacteria) can degrade cellulose by the intervention of extracellular enzymes known as cellulases. Cellulases catalyze the hydrolysis of cellulose chains leading to a decrease of their degree of polymerization and to an increase of free glucose content [32]. Consequently, paper aging and degradation compromise its mechanical properties. In the absence of microorganisms, other attacks comprehend the lowering of pH and chemical oxidation. These processes are caused by interaction with environment, light, and oxygen. All these chemical changes further catalyze the degradation of cellulose. Despite this, the paper spontaneous biodegradation is usually testified in support of the environmental harmlessness of paper electronics: at the end of the device lifetime, the paper substrate can be degraded and the internal and precious device layers can be safely recovered [33]. Alternatively, incineration of the device represents a good way to safely dispose a paper-supported device [34, 35]. However, no systematic studies have been performed clarifying whether the lifetime of different forms of paper (including nanopapers) is compatible with the expected lifetime of thin film devices.

2.2. CNP as Substrate for Solar Cells. The high potentialities shown by nanopaper for electrode deposition have turned on a relevant interest in the demonstration of optoelectronic devices deposited on CNP. Devices like solar cells would highly benefit from the controllable haze offered by nanopaper that potentially allows increasing the light path into the active layers of the device. Examples of polymer [11, 12, 21, 35–38] and perovskite [39] solar cells deposited on cellulose nanopaper have already appeared on the literature.

Zhou et al. [35] demonstrated a polymer solar cell with an inverted geometry deposited on a CNCs nanopaper with an average surface roughness of 1.8 ± 0.6 nm (Figures 6(a)–6(e)). The substrate was prepared by casting a 2% w/w suspension of CNCs in distilled water in a polystyrene petri dish. Due to the high hygroscopic character of the nanopaper, it is not compatible with deposition of active materials from water-containing solutions: the transparent cathode could not be deposited by applying pastes or spin-coating materials provided as water solutions, like PEDOT:PSS for instance. For this reason, a 20 nm thick layer of Ag was evaporated on the nanopaper as bottom electrode. A device with the geometry nanopaper/Ag/PEIE/PBDTTT-C:PCBM/MoO_3/Ag (Figures 6(a)–6(c)) was realized and yielded an energy conversion efficiency under illumination with an AM 1.5 field of $2.7 \pm 0.1\%$.

The nanopaper prepared from CNCs promptly disaggregated in water. Zhou et al. demonstrated how this characteristic could be exploited to recover the cellulose nanocrystals and the device layers by immersion of the device, at the end of its use, in sequences of different solvents with water as first solvent. Water was reported to completely resuspend the cellulose nanocrystals within 30 minutes. This finding suggests that nanopaper prepared from CNCs, due to its high hygroscopicity, may not be the ideal substrate for organic solar cells. Moreover, nanopaper can present a not negligible water vapour transmission rate, a characteristic that may compromise the device active layers. In addition, immediate problems of shape stability of nanopaper need to be faced upon its exposure to ambient moisture. These aspects represent limiting issues for the real application of devices deposited on nanopaper, including solar cells. This motivates the birth of a research field on the reengineering of the properties of paper and nanopaper, with the aim to enable access to more reliable transparent thin films with preserved sustainability and thermal and mechanical stabilities and, in addition, showing encapsulant and barrier properties.

3. Reengineering of Cellulose Nanopaper by Chemical Design

3.1. Chemical Manipulation of Cellulose Nanopaper. Topochemical functionalization [40] on nanopaper can help to decrease the water vapour transmission rate across the nanopaper thin film. A topochemical functionalization on crystalline cellulose is limited to the groups present in the accessible regions of the nanopaper thin films, i.e., only the surface of the nanofibres. The topochemical approach involves only the surface of the crystalline celluloses and differs from bulk functionalization that proceeds through dissolution of the crystalline structure accompanied by complete derivatization. The topochemical approach requires the adoption of very mild reaction conditions: the functionalization must interest only the most reactive pending hydroxyl groups on the surface of the nanocelluloses and does not have to compromise their crystalline structure. For this reason, the use of swelling media and of reaction conditions able to activate the peeling off of the surface cellulose chains forming the crystalline structure should be avoided. With this respect, CNCs and CNFs are high aspect ratio crystalline organic nanoparticles with abundant surface alcohol groups (Figure 7(b)). The pending functionalities derive from the chemical structure of the cellulose polymer that can formally be considered as a sequence of the disaccharide cellobiose (Figure 7(a)). The protruding alcohol (primary or secondary) groups on the surface of the nanocrystals are amenable of chemical manipulation. This allows to finely modulate the properties not only of the crystalline cellulose but also of the

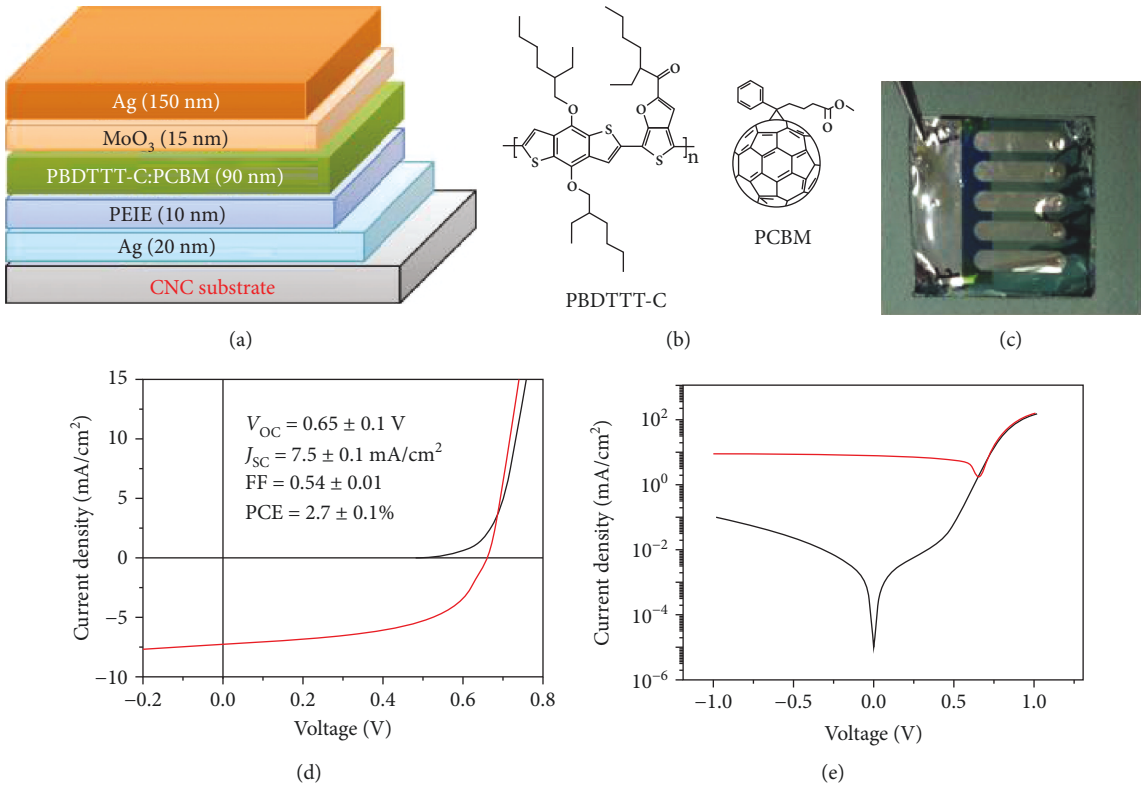

Figure 6: (a) Device architecture of a polymer solar cell deposited on CNC nanopaper. The evaporation of a thin layer of Ag allows deposition of the bottom electrode that was then modified through a thin layer of ethoxylated polyethylenimine (PEIE); (b) chemical structure of the active materials. PBDTTT-C: poly[(4,8-bis-(2-ethylhexyloxy)-benzo[1,2-b:4,5-b9]dithiophene)-2,6-diyl-alt-(4-(2-ethylhexanoyl)-thieno[3,4-b]thiophene)-2,6-diyl], polymer donor; PCBM: phenyl-C61-butyric acid methyl ester, molecular acceptor; (c) a photograph of the polymer solar cell deposited on nanopaper; (d) JV characteristics of the solar cell in the dark (black) and under illumination on the nanopaper side (red); (e) JV characteristics in a semilogarithmic scale. Reproduced from reference [35] with permission from Springer Nature.

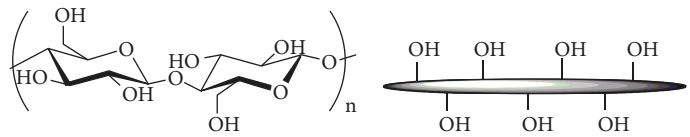

Figure 7: (a) Chemical structure of cellulose polymer; (b) representation of a cellulose nanofibre or nanocrystal: a rod with abundant free surface pending -OH (primary or secondary) groups.

nanopaper. Some studies have shown that attaining a very low degree of substitution of the cellulose polymer (DS < 0.37) preserves the cellulose crystallinity [41]. In principle, the primary alcohol pendant groups are more reactive than the secondary ones and more available for topochemical functionalization. However, some studies have shown that functionalization often proceeds involving all the available surface hydroxyl groups, i.e., the one linked to C_6, and the secondary ones linked to C_2 and C_3 carbon atoms of each β-D-glucopyranosidic ring [42, 43].

Some strategies for the topochemical functionalization of nanopaper have been proposed, with the aim of increasing the water stability or decreasing the water vapour transmission rate of nanopaper. Some studies have focalized only on the modification of paper and on the in-depth characterization of the effects on its surface and bulk properties, taking into consideration, as well, cellulose crystallinity. Other studies have been sided also by a device demonstrator.

One of the first reports along this direction was published by Cunha et al. [44], who have studied the effect of topochemical acetylation on cellulose nanopaper. CNP was prepared from CNFs or from bacterial cellulose by the vacuum filtration method. The acetylation was carried out dipping the nanopaper in a solution prepared with one equivalent of acetic anhydride with respect to the total free -OH group content of the nanopaper in toluene solvent and few drops

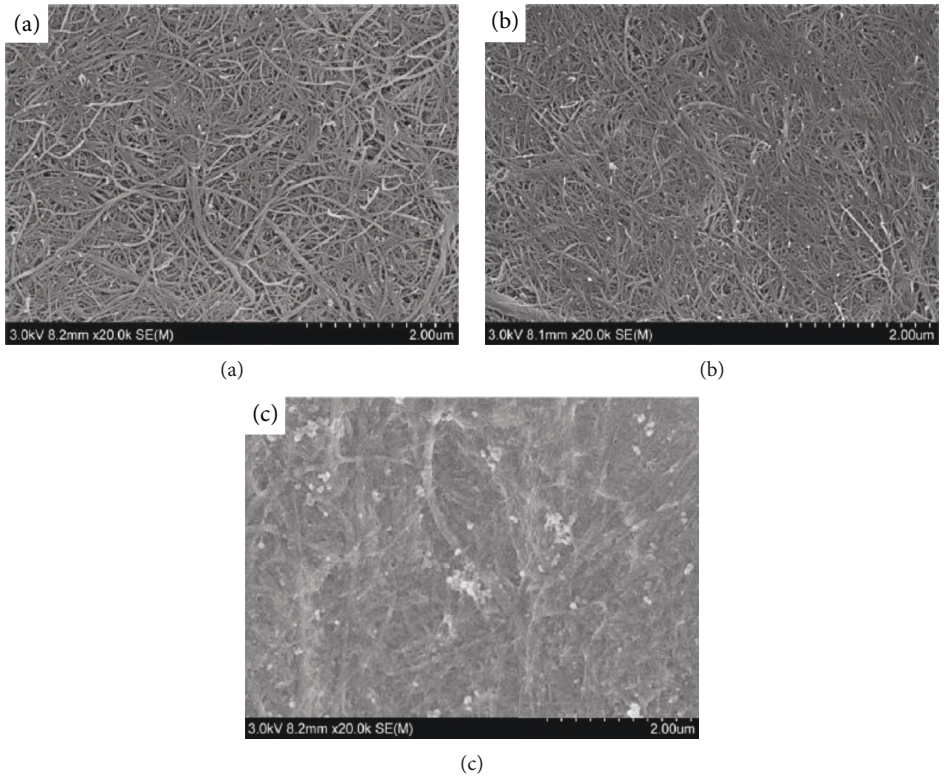

Figure 8: (a) FE-SEM surface micrographs of as prepared CNF nanopaper; (b) the same nanopaper after reaction with acetic anhydride (Ac_2O); (c) the same nanopaper after overacetylation. Reproduced from reference [44] with permission from Springer.

of concentrated H_2SO_4 as catalyst. By attaining, on average, low degrees of substitution on their samples, the authors demonstrated that the reaction did not affect the nanopaper morphology and overall crystallinity. Figures 8(a) and 8(b) show the FE-SEM micrographs of the CNF nanopaper before and after the topochemical functionalization. In these samples, the water sorption mechanism of the nanopaper started with hydration of the nanocelluloses surface. Actually, the water sorption was apparently sensitively decreased after the topochemical functionalization, but the nanocellulose acetylation reaction conditions needed to be finely controlled, because an overfunctionalization of the fibres induced uncontrolled swelling of the nanofibres. The excessive functionalization caused loss of crystallinity and degradation of mechanical properties of the nanopaper.

Along this direction, water stable nanopaper was achieved by surface chemical functionalization with lauroyl chloride [45]. In this work, a CNC nanopaper was prepared by solution casting nanocrystals isolated by acid hydrolysis, the same procedure described in the paragraph 2.2 and reported by Zhou et al. The pristine nanopaper was subjected to surface hydrophobization by dipping in a solution of acyl chlorides in dichloromethane containing pyridine as catalyst (Figure 9(a)), yielding hydrophobized nanopaper that was named C_{12}-CNP. In this case and differently from the previous example reported by Cunha et al., the more film-like appearance of the CNP surface (Figure 9(b)) due to the very tiny cellulose nanocrystals used for the production of the nanopaper was expected to limit the functionalization to the surface of the nanopaper itself due to hindered penetration of the reactants inside CNP. The reaction yielded a very low DS (0.034), calculated from elemental analyses. Probing the surface of the nanopaper by XRD technique confirmed a limited surface reorganization, with preserved cellulose I crystalline structure. The surface esterification changed the nanopaper properties, producing a hydrophobized C_{12}-CNP with a surface water contact angle of $114 \pm 6^\circ$. Atomic force microscopy topographies demonstrated preserved aggregation patterns and textures of the surface of the nanopapers (Figures 9(b) and 9(c)), with slightly "swelled" surface CNCs. This was attributed to the presence of lauroyl functional groups attached to the surface of CNCs and increasing their diameter. A similar behavior was observed on other H-bonded organic nanoparticles [46]. In spite of such a little change observed in morphological properties, the water resistance was dramatically increased: two orders of magnitude decrease in bulk porosity was detected electrochemically in C_{12}-CNP that, differently from pristine CNP, was stable for hours upon immersion in electrolyte water solution.

Another nanopaper modification was performed via octadecyltrichlorosilane (OTS) surface treatment to reduce its vulnerability to humidity and moisture. The modified nanopaper was used as substrate for perovskite solar cells [39], whose performances can be drastically tampered by moisture. The treatment was performed for 30 s with a 0.1 M solution of OTS and yielded a hydrophobic nanopaper with a surface water contact angle of 103°. After that, a TiOx/Ag/TiOx DMD (dielectric-metal-dielectric) multilayer

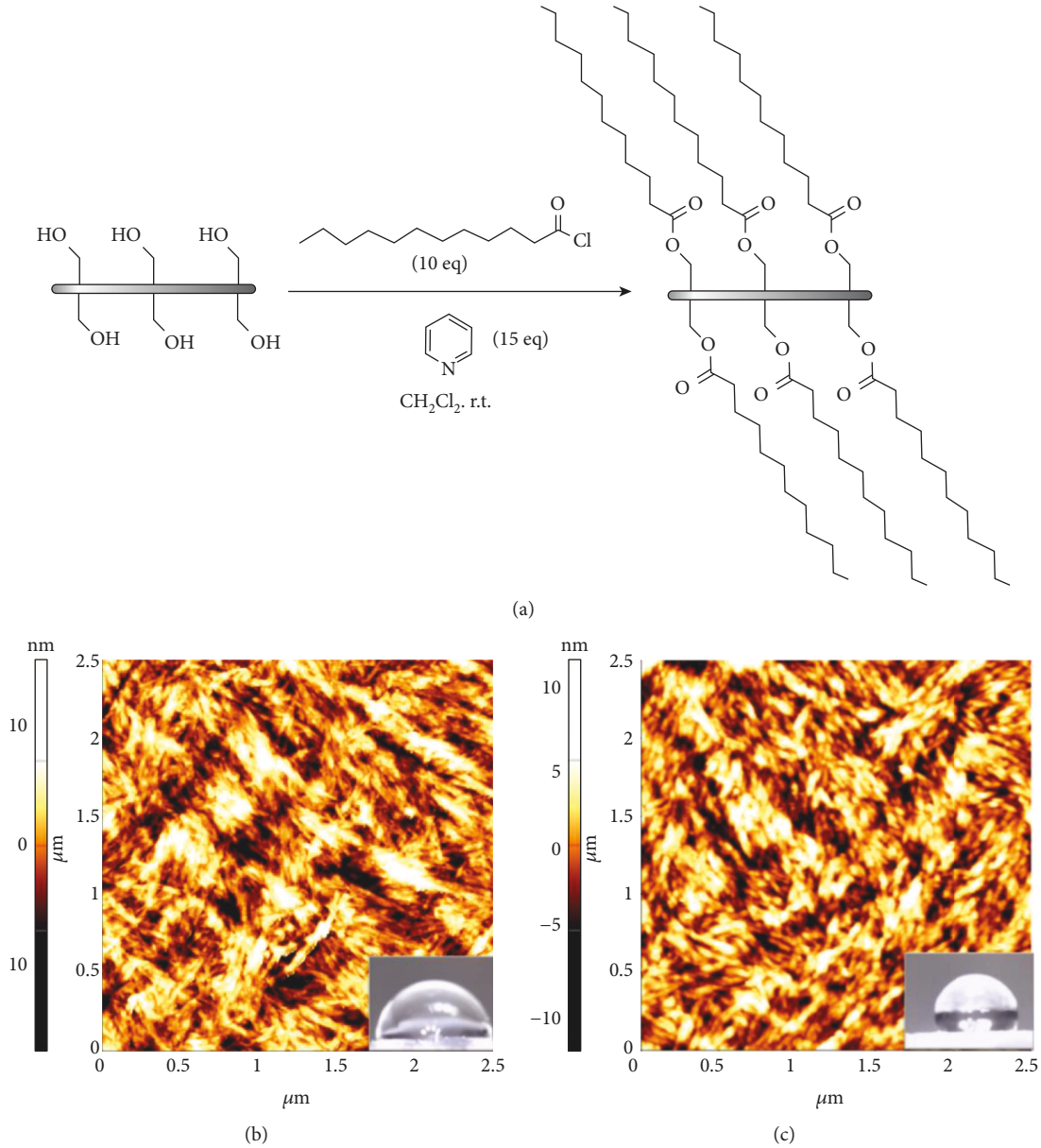

Figure 9: (a) Topochemical hydrophobization of CNP produced by dipping in lauroyl chloride solutions, with pyridine as catalyst. The reaction produces nanopaper with a very low DS (<0.1); (b) AFM $2.5 \times 2.5\,\mu m^2$ topography of the surface of pristine nanopaper. Inset: water contact angle on pristine nanopaper; (c) AFM $2.5 \times 2.5\,\mu m^2$ topography of the surface of hydrophobized nanopaper. Inset: water contact angle on hydrophobized nanopaper, C_{12}-CNP. Reproduced from reference [45] with permission from the Royal Society of Chemistry.

electrode was grown on the nanopaper by sputtering deposition technique. This allowed the preparation of multilayer photovoltaic devices with a series of perovskites ($CH_3NH_3PbI_{3-x}Br_x$) in the active layer and Spiro-OMeTAD as hole transport material with a maximum efficiency of 6.37%. Figure 10 shows the model crystal structure of $CH_3NH_3PbI_3$, the best performing active layer, the device architecture, and a SEM cross-section of the device, evidencing the presence of all the different layers deposited on the nanopaper.

A highly transparent and hazy CNP endowed with a self-cleaning superhydrophobic surface (static water contact angle 159.6°) was attained via cellulose silanization [47]. The nanopaper was composed of TEMPO-oxidized cellulose nanofibrils (TOCNF), prepared via vacuum filtration. The polysiloxanes were polymerized on the surface of the nanopaper in situ, forming a 3D network grafted to the nanopaper *via* siloxane linkages (Figures 11(a) and 11(b)). The modified nanopaper was superhydrophobic (Figure 11(d)), but still, it possessed high transparency and haze (Figure 11(e)) and could be used as a coating layer for a polysilicon solar cell. Due to its superhydrophobic nature, water and dust showed very poor adhesion on its surface. This was fundamental, because dust could not deposit on the solar cell and hamper the efficiency of its illumination. The high haze and transparency of

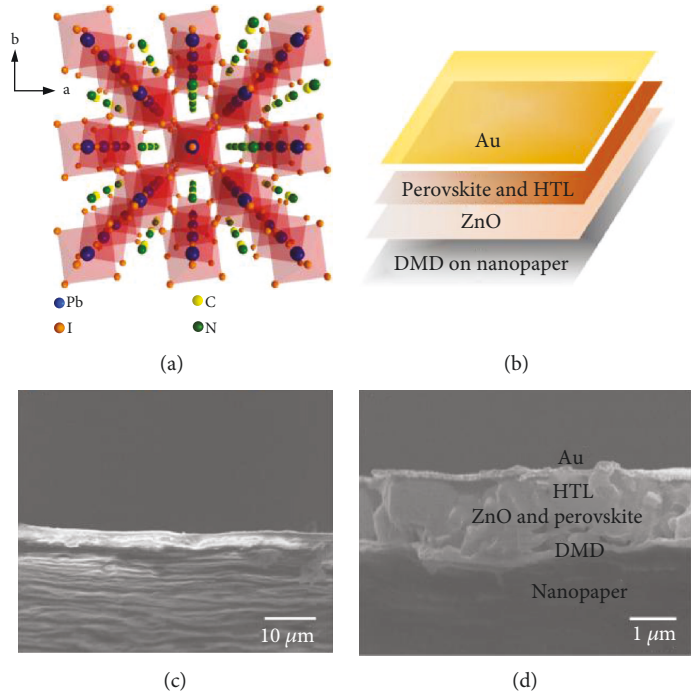

FIGURE 10: (a) Representation of the crystalline structure of $CH_3NH_3PbI_3$; (b) solar cell device architecture deposited on nanopaper; (c, d) SEM micrographs representing the cross-section of the device layers with scale bar 10 μm and 1 μm, respectively. Device architecture: nanopaper/DMD/ZnO layer with $CH_3NH_3PbI_3$/Spiro-OMeTAD/Au. Reproduced from reference [39] with permission from Elsevier.

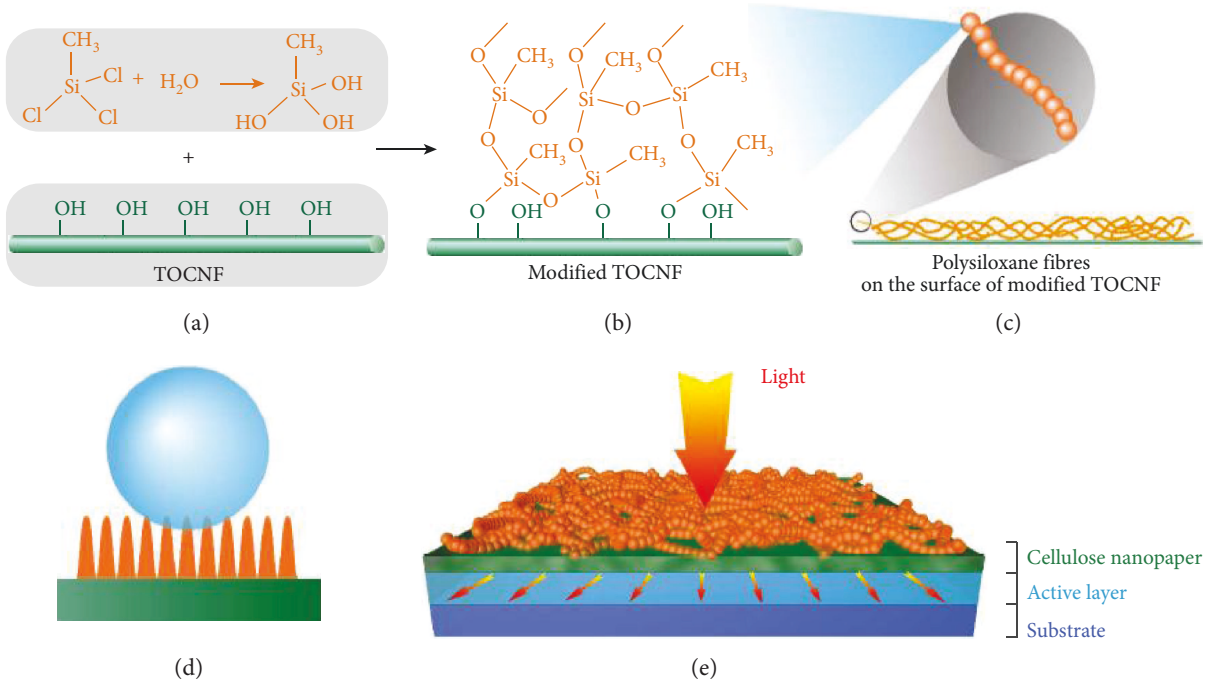

FIGURE 11: Tempo-oxidized cellulose nanofibril paper modified with polysiloxanes (a–c). The polysiloxane fibres transform the nanopaper into a superhydrophobic surface (d). The cellulose nanopaper is transparent and presents high haze and was used to optimize the performance of a solar cell (e). Reproduced from reference [47] with permission from the American Chemical Society.

the superhydrophobic nanopaper coating layer allowed to detect power conversion efficiencies as high as 11.48%, with an enhancement of performances of 14% with respect to the bare cell.

Another strategy to increase the stability of nanopaper was based on chemical cross-linking. CNP with shape stability upon contact with water was obtained by cross-linking with glutaraldehyde [48]. Cross-linking occurred

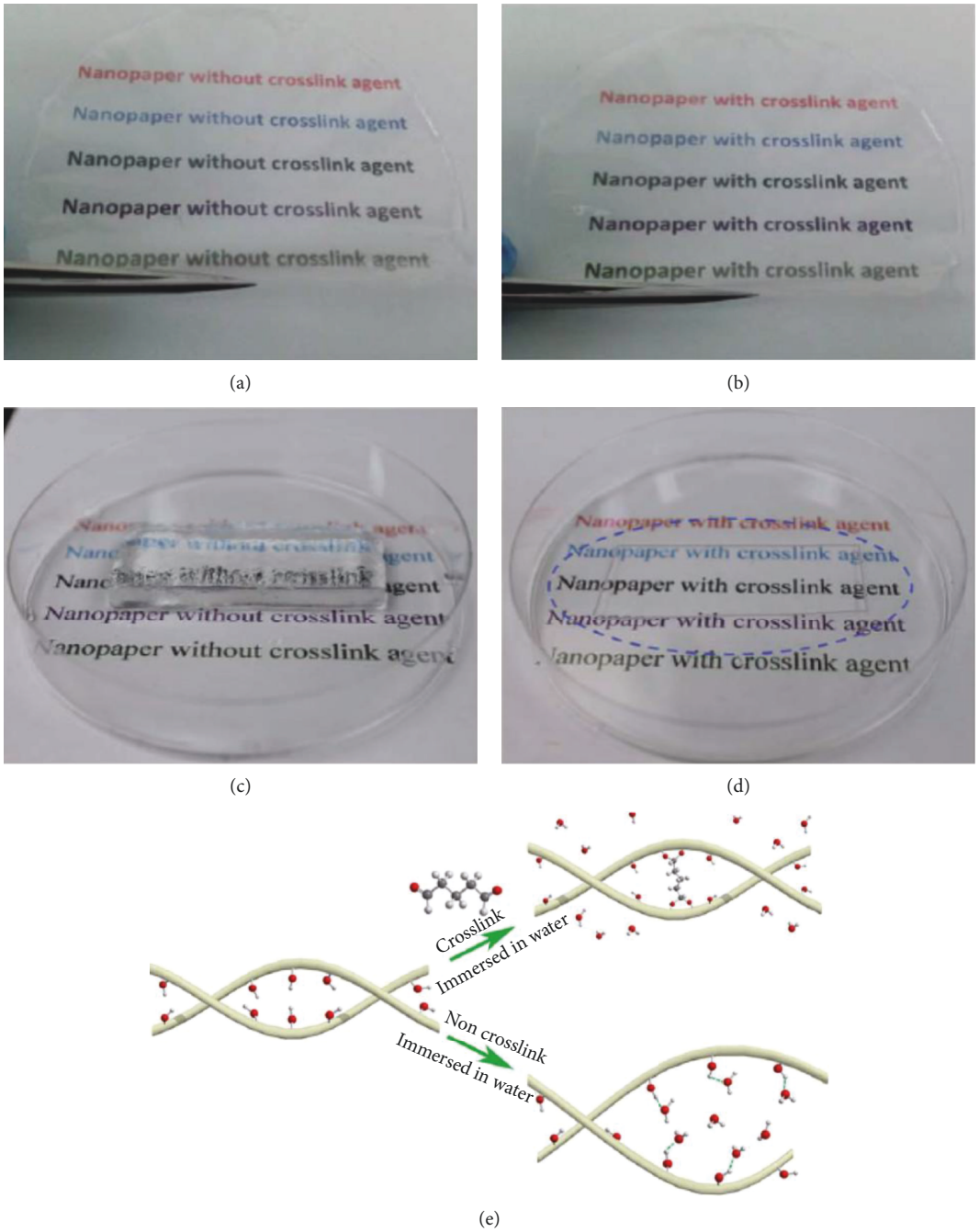

Figure 12: (a) Pristine nanopaper before the cross-linking treatment. (b) Nanopaper after the cross-linking treatment. (c) Pristine nanopaper after immersion in water for 24 h. The thickness of the nanopaper expanded from 30 μm to 6 mm. (d) Cross-linked nanopaper immersed in water for 24 h. (e) Schematic representation of the shape stability improvement attained after glutaraldehyde treatment. Reproduced from reference [48] with permission from the Royal Society of Chemistry.

when the cellulose nanomaterials were mixed with glutaraldehyde in an acid environment. The cross-linked nanopaper did not swell upon exposure for 24 hours to water (Figures 12(b) and 12(d)) and was compatible with the gravure printing process of active inks. Figure 12(e) shows the effects of the use of glutaraldehyde as the cross-linking agent: by forming acetals on the nanocrystal surface (Figure 12(e)), it acts as a cross-linker, hinders the exposure of hydroxyl groups to the solvent, fixes the distance between different fibres reducing their mobility, and improves the shape stability of nanopaper in water.

3.2. Tailoring Properties via Composites. Another approach to hydrophobize CNP consists in blending the nanocelluloses with a second material. The treatment should not compromise the transparency of CNP.

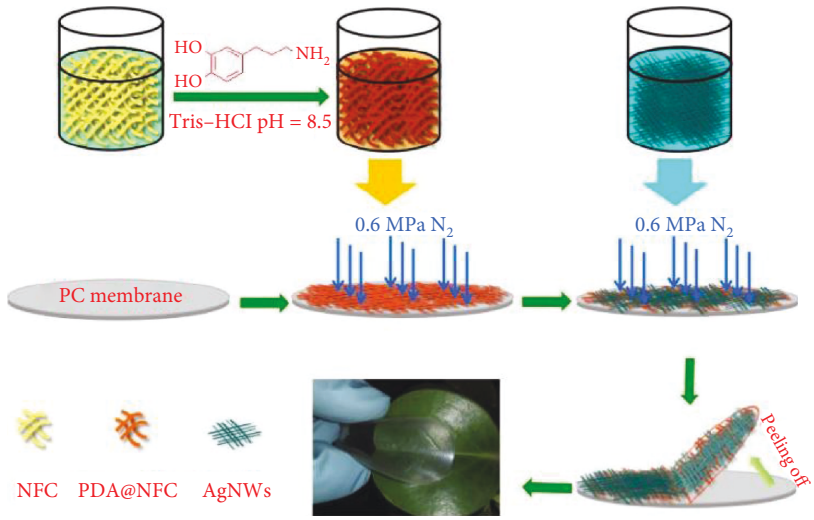

Figure 13: Preparation of polydopamine modified nanopaper. A solution of cellulose nanofibres (yellow) is additivated with dopamine at controlled pH. After polymerization, the solution turns brown. A polydopamine-cellulose nanopaper is produced by the filtration method. Using the same method, a thin AgNW (blue-green) conductive layer is deposited on the surface of the PDA nanopaper. Reproduced from reference [49] with permission from the Royal Society of Chemistry.

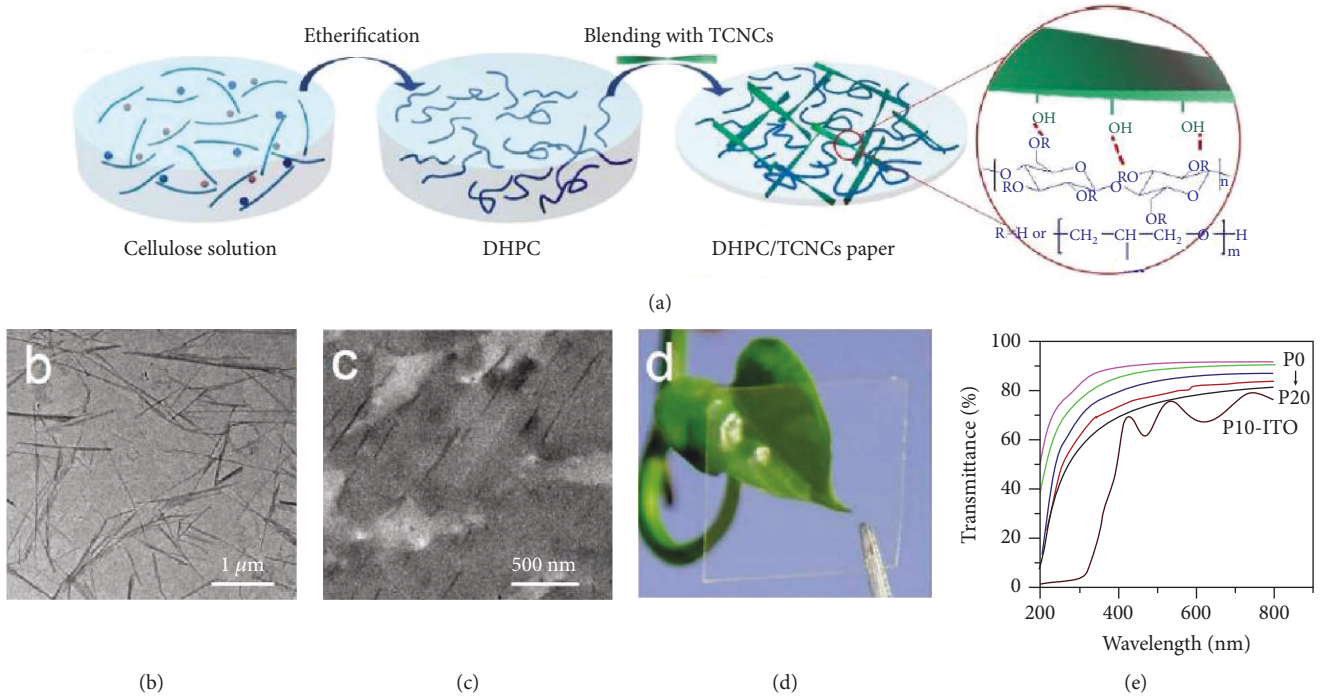

Figure 14: (a) Fabrication of cellulose-based nanocomposite papers: etherification of cellulose to synthesize DHPC, followed by blending with tunicate CNCs and filtering. The cellulose ether interacts with the cellulose nanocrystal surface by accepting H-bonds. (b) TEM image of CNCs (scale bar: 1 μm); (c) TEM image of composite films (scale bar: 500 nm); (d) photograph of the composite film and (e) optical transmittance in the UV-Vis region of nanocomposite papers at different DHPC content. Reproduced from reference [12] with permission from the American Chemical Society.

Modification of CNP with a semitransparent material was achieved by self-polymerization of dopamine on the surface of the nanocrystals at controlled pH before the nanopaper deposition (Figure 13). The polydopamine (PDA) layer adheres to the nanofibre surface and works as an adhesive network. Ag nanowires (AgNWs) can be mixed with the two materials as well and can be used to make the CNP conductive [49]. Polydopamine forms a network around the nanofibrillated cellulose that reinforces the nanopaper: the stress-strain behavior improved in the order

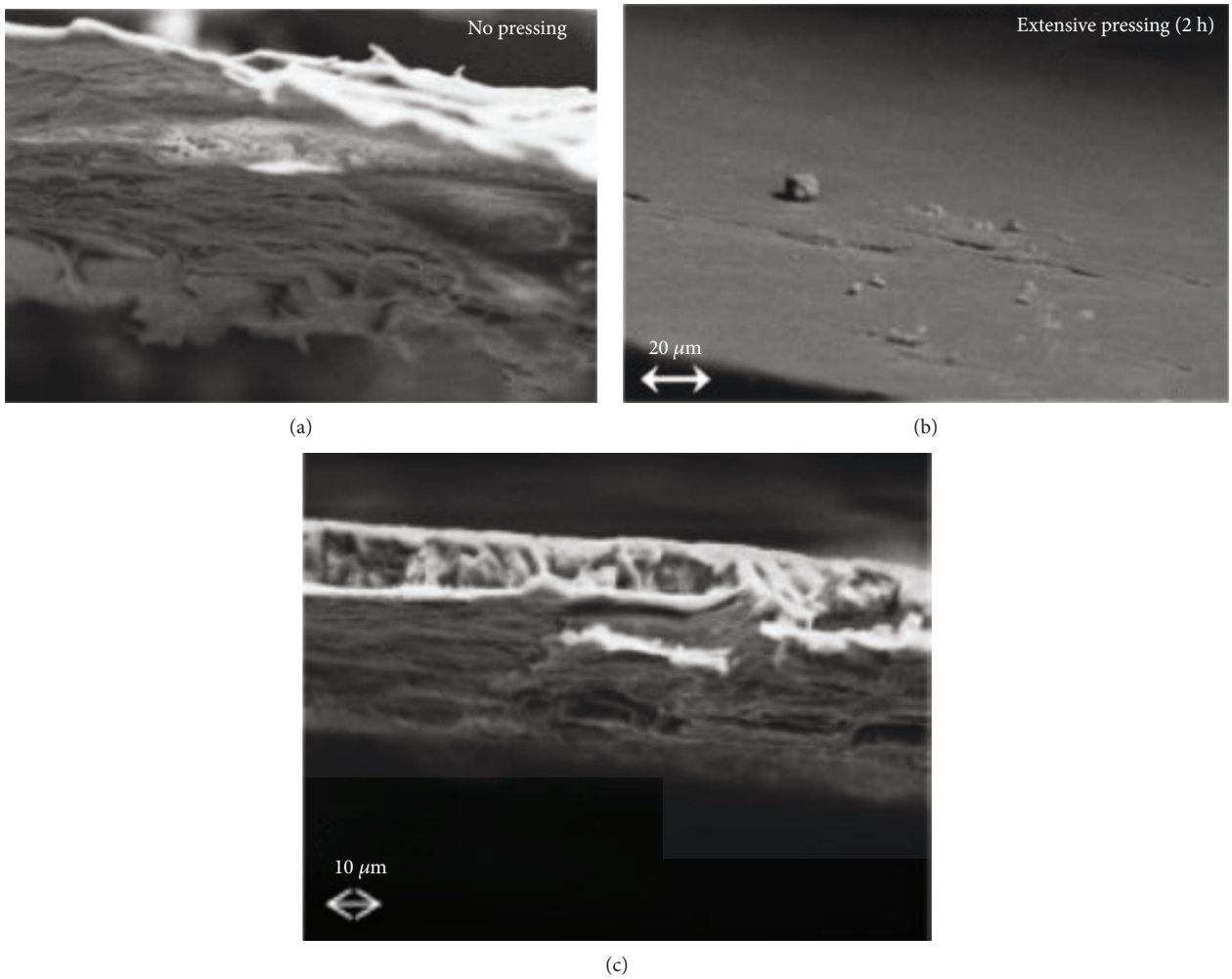

Figure 15: FE-SEM micrographs of cellulose nanofibre nanopaper sections acquired: (a) on pristine nanopaper; (b) after hot-pressing for two hours; (c) after hot-pressing and deposition of a paraffin wax on nanopaper surface. Reproduced from reference [50] with permission from the American Chemical Society.

CNP < PDA@CNP < AgNWs@PDA@CNP. Moreover, the new composite possessed outstanding air and chemical corrosion stabilities, showing unvaried properties after being exposed in air for 150 days or immersed in different solutions for 180 minutes. In particular, resistance upon immersion in strong acid solution (HNO_3, pH 3), strong alkaline solution (NaOH, 4 wt%), neutral salt solution (NaCl, 4 wt%), and strong alkaline salt solution (Na_2S, 4 wt%) was tested.

New transparent all cellulose-based nanocomposite papers were attained by blending stiff tunicate cellulose nanocrystals with *O*-(2, 3-dihydroxypropyl) cellulose (DHPC) [12]. DHCP self-standing films lacked the necessary tensile strength and toughness which are necessary for using them as substrates for solar cells. Conversely, the use of an "all cellulose" nanocomposite showed good mechanical strength while retaining overall sustainability of the material. The process for the preparation of the nanocomposites is shown in Figure 14. First, the DHCP polymer was synthesized in solution by an etherification process. After that, the polymer was blended with the cellulose nanocrystals. The CNCs from tunicate displayed very good dispersibility in the DHPC matrix, thanks to H-bond donation from the surface alcohol groups of tunicate CNCs to the ether groups of DHCP (Figure 14(a)) that yielded a nanocomposite with very good mechanical properties. The composites were transparent and could be used as substrates for flexible bulk-heterojunction polymer solar cells fabricated in the inverted geometry, with a blend formed by the low bandgap polymer P7B7 and PCBM in the active layer. The solar cell remarkably displayed a power conversion efficiency of 4.98%.

A further approach to produce hydrophobized CNF nanopaper was described by Österberg et al. [50]. They used overpressure filtration and hot-pressing for fast drying of CNF films. The FE-SEM micrograph of a CNF nanopaper section before and after two hours of hot-pressing is shown in Figures 15(a) and 15(b). A much smoother surface is produced with the pressure treatment. The hot-pressed films were robust and resistant to many solvents for almost 24 hours, and this opened to new surface functionalization. In particular, deposition of a hydrophobic wax was taken into consideration: the wax used was cheap and paraffin based, and the modified films were supposed to

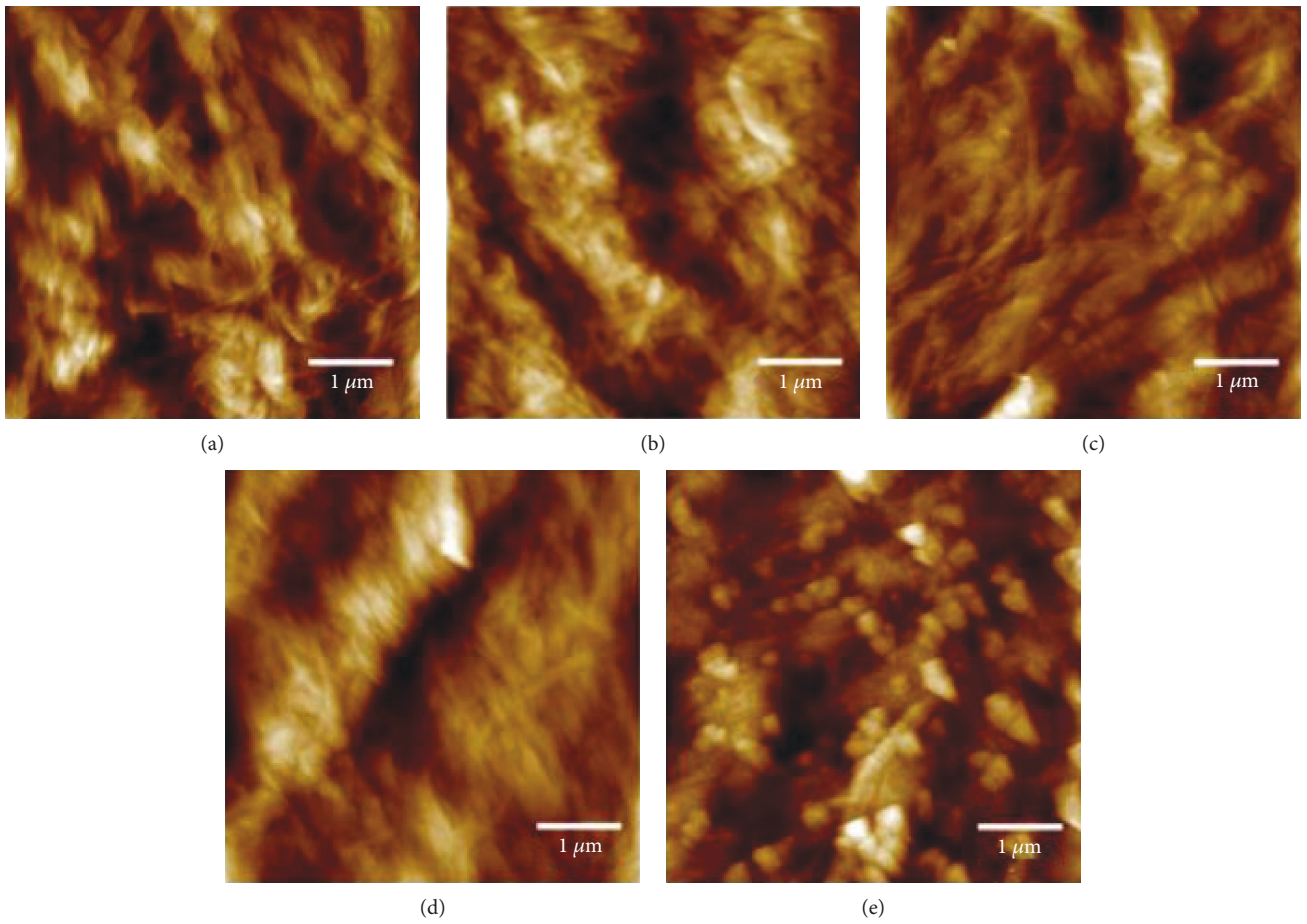

Figure 16: 5 × 5 μm AFM topographies of bacterial nanofibre paper: (a) on pristine sample; after adsorption of (b) polystyrene from toluene, (c) polystyrene from toluene/heptane, (d) poly(trifluoroethylene) from THF, and (e) poly(trifluoroethylene) from THF/toluene. Reproduced from reference [51] with permission from the American Chemical Society.

resist to a high humidity environment. Indeed, the treatment preserved the strength of the film while both oxygen transmission and water vapour transmission rates were decreased considerably. Moreover, the water contact angle increased from 40° to 110° upon wax deposition yielding a hydrophobic surface.

In a work by Kontturi et al. [51], simple exposure of nanopapers to nonaqueous aprotic solutions of hydrophobic polymers resulted in adsorption of these materials on bacterial cellulose nanofibre paper surface and controlled surface modification towards water repellence. As polymers, the well-known polystyrene and poly(trifluoroethylene) were chosen, deposited from solvent/nonsolvent mixtures. Toluene was a good solvent for both materials and could allow absorption of the lowest amount of polymers. The use of solvent/-nonsolvent mixtures increased the yield of deposition. AFM topographies, reproduced in Figures 16(b)–16(e), showed retention of nanofibre surface aggregation patterns with respect to the pristine nanopaper (Figure 16(a)), indicative of negligible alterations of surface morphologies after molecular adsorption. Only the samples with the highest amount of poly(trifluoroethylene) on the surface (Figure 16(e)) showed the appearance of aggregates. The modified nanopapers were water repellent, but their water vapour uptake properties was unaffected by the treatment. Evidently, the two polymers were not able to penetrate the nanopaper pores. Another criticism is given by the nonbiodegradable nature of the materials used for the surface modification.

4. Conclusions

Cellulose nanopaper, in view of its remarkable features, promises to enable new applications that could not be even envisaged for standard paper, with promising perspectives in particular in flexible electronics and light-harvesting devices. However, its high hygroscopicity introduces some issues, like the necessity of protecting the device layers from the cellulose natural attitude to adsorb water. For this reason, a completely new chemical design is needed to reengineer the nanopaper properties. Some strategies have already been proposed, even if only few studies have faced systematically the problem so far. The present literature proposes (i) to modify the nanopaper properties by topochemical functionalization or (ii) to attain all cellulose or biodegradable nanocomposites to increase the nanopaper resistance

to humidity. These are convenient and straightforward approaches to cellulose nanopaper with chemically tailored properties but, in case of being accompanied by a decrease of the cellulose crystallinity, could negatively impact the properties of the composite nanopapers. More in-depth studies will be needed in the future to better assess the effects of the chemical manipulation on the stability and properties of cellulose nanopaper.

Conflicts of Interest

The author declares that there is no conflict of interest regarding the publication of this paper.

Acknowledgments

This work was financially supported by Regione Puglia, program FutureInResearch, project "SolarLeaf - Biodegradable organic solar cells supported on cellulose (Prot. F6YRA01)" and by Universita degli Studi di Bari Aldo Moro.

References

[1] A. Payen, "Mémoire sur la composition du tissu propre des plantes et du ligneux," *Comptes Rendus*, vol. 7, pp. 1052–1056, 1838.

[2] D. Klemm, B. Philipp, T. Heinze, U. Heinze, and W. Wagenknecht, *Comprehensive Cellulose Chemistry: Fundamentals and Analytical Methods*, WILEY-VCH Verlag GmbH, Weinheim, 1998.

[3] Data from CEPI, RISI, AF&PA, JPA, PPC, "Bracelpa," 2015, http://www.assocarta.it.

[4] R. Das, X. He, and K. Ghaffarzadeh, "Printed, organic & flexible electronics forecasts," in *Players & Opportunities 2017-2027*, IDTechEx, 2017.

[5] D. Tobjörk and R. Österbacka, "Paper electronics," *Advanced Materials*, vol. 23, no. 17, pp. 1935–1961, 2011.

[6] F. Brunetti, A. Operamolla, S. Castro-Hermosa et al., "Printed solar cells and energy storage devices on paper substrates," *Advanced Functional Materials*, vol. 29, no. 21, article 1806798, 2019.

[7] L. Ren'ai, K. Zhang, G. Chen et al., "Green polymerizable deep eutectic solvent (PDES) type conductive paper for origami 3D circuits," *Chemical Communications*, vol. 54, no. 18, pp. 2304–2307, 2018.

[8] Y. Yao, J. Tao, J. Zou et al., "Light management in plastic-paper hybrid substrate towards high-performance optoelectronics," *Energy & Environmental Science*, vol. 9, no. 7, pp. 2278–2285, 2016.

[9] M. He, K. Zhang, G. Chen, J. Tian, and B. Su, "Ionic gel paper with long-term bendable electrical robustness for use in flexible electroluminescent devices," *ACS Applied Materials & Interfaces*, vol. 9, no. 19, pp. 16466–16473, 2017.

[10] W. Hu, G. Chen, Y. Liu, Y. Liu, B. Li, and Z. Fang, "Transparent and hazy all-cellulose composite films with superior mechanical properties," *ACS Sustainable Chemistry & Engineering*, vol. 6, no. 5, pp. 6974–6980, 2018.

[11] Z. Fang, H. Zhu, Y. Yuan et al., "Novel nanostructured paper with ultrahigh transparency and ultrahigh haze for solar cells," *Nano Letters*, vol. 14, no. 2, pp. 765–773, 2014.

[12] Q. Cheng, D. Ye, W. Yang et al., "Construction of transparent cellulose-based nanocomposite papers and potential application in flexible solar cells," *ACS Sustainable Chemistry & Engineering*, vol. 6, no. 6, pp. 8040–8047, 2018.

[13] M. Nogi, S. Iwamoto, A. N. Nakagaito, and H. Yano, "Optically transparent nanofiber paper," *Advanced Materials*, vol. 21, no. 16, pp. 1595–1598, 2009.

[14] A. Barhoum, P. Samyn, T. Öhlund, and A. Dufresne, "Review of recent research on flexible multifunctional nanopapers," *Nanoscale*, vol. 9, no. 40, pp. 15181–15205, 2017.

[15] F. Hoeng, A. Denneulin, and J. Bras, "Use of nanocellulose in printed electronics: a review," *Nanoscale*, vol. 8, no. 27, pp. 13131–13154, 2016.

[16] *TAPPI Standards: Regulations and Style Guidelines, Standard Terms and Their Definition for Cellulose Nanomaterials*W 13021.

[17] H. Sehaqui, T. Zimmermann, and P. Tingaut, "Hydrophobic cellulose nanopaper through a mild esterification procedure," *Cellulose*, vol. 21, no. 1, pp. 367–382, 2014.

[18] Y. Habibi, A.-L. Goffin, N. Schiltz, E. Duquesne, P. Dubois, and A. Dufresne, "Bionanocomposites based on poly(ε-caprolactone)-grafted cellulose nanocrystals by ring-opening polymerization," *Journal of Materials Chemistry*, vol. 18, no. 41, pp. 5002–5010, 2008.

[19] H. Kargarzadeh, I. Ahmad, S. Thomas, and A. Dufresne, Eds., *Handbook of Nanocellulose and Cellulose Nanocomposites*, Wiley-VCH Verlag GmbH & Co. KGaA, 2017.

[20] Z. Fang, H. Zhu, W. Bao et al., "Highly transparent paper with tunable haze for green electronics," *Energy & Environmental Science*, vol. 7, no. 10, pp. 3313–3319, 2014.

[21] L. Hu, G. Zheng, J. Yao et al., "Transparent and conductive paper from nanocellulose fibers," *Energy & Environmental Science*, vol. 6, no. 2, pp. 513–518, 2013.

[22] H. Zhu, Z. Fang, C. Preston, Y. Li, and L. Hu, "Transparent paper: fabrications, properties, and device applications," *Energy & Environmental Science*, vol. 7, no. 1, pp. 269–287, 2014.

[23] Y. Fujisaki, H. Koga, Y. Nakajima et al., "Transparent nanopaper-based flexible organic thin-film transistor array," *Advanced Functional Materials*, vol. 24, no. 12, pp. 1657–1663, 2014.

[24] H. Fukuzumi, T. Saito, Y. Okita, and A. Isogai, "Thermal stabilization of TEMPO-oxidized cellulose," *Polymer Degradation and Stability*, vol. 95, pp. 1502–1508, 2010.

[25] J. Chen, M. Akin, L. Yang et al., "Transparent electrode and magnetic permalloy made from novel nanopaper," *ACS Applied Materials & Interfaces*, vol. 8, no. 40, pp. 27081–27090, 2016.

[26] N. Lin and A. Dufresne, "Surface chemistry, morphological analysis and properties of cellulose nanocrystals with gradiented sulfation degrees," *Nanoscale*, vol. 6, no. 10, pp. 5384–5393, 2014.

[27] A. Punzi, A. Operamolla, O. Hassan Omar et al., "Designing small molecules as ternary energy-cascade additives for polymer:fullerene solar cell blends," *Chemistry of Materials*, vol. 30, no. 7, pp. 2213–2217, 2018.

[28] M. C. Hsieh, C. Kim, M. Nogi, and K. Suganuma, "Electrically conductive lines on cellulose nanopaper for flexible electrical devices," *Nanoscale*, vol. 5, no. 19, pp. 9289–9295, 2013.

[29] H. Fukuzumi, T. Saito, T. Iwata, Y. Kumamoto, and A. Isogai, "Transparent and high gas barrier films of cellulose nanofibers

prepared by TEMPO-mediated oxidation," *Biomacromolecules*, vol. 10, no. 1, pp. 162–165, 2009.

[30] S. S. Nair, J. Zhu, Y. Deng, and A. J. Ragauskas, "High performance green barriers based on nanocellulose," *Sustainable Chemical Processes*, vol. 2, no. 1, 2014.

[31] M. Henriksson, L. A. Berglund, P. Isaksson, T. Lindström, and T. Nishino, "Cellulose nanopaper structures of high toughness," *Biomacromolecules*, vol. 9, no. 6, pp. 1579–1585, 2008.

[32] L. Micheli, C. Mazzuca, A. Palleschi, and G. Palleschi, "Combining a hydrogel and an electrochemical biosensor to determine the extent of degradation of paper artworks," *Analytical and Bioanalytical Chemistry*, vol. 403, pp. 1485–1489, 2012.

[33] Y. H. Jung, T.-H. Chang, H. Zhang et al., "High-performance green flexible electronics based on biodegradable cellulose nanofibril paper," *Nature Communications*, vol. 6, no. 1, article 7170, 2015.

[34] S. Castro-Hermosa, J. Dagar, A. Marsella, and T. M. Brown, *IEEE Electron Device Letters*, vol. 38, no. 9, pp. 1278–1281, 2017.

[35] Y. Zhou, C. Fuentes-Hernandez, T. M. Khan et al., "Recyclable organic solar cells on cellulose nanocrystal substrates," *Scientific Reports*, vol. 3, no. 1, pp. 24–26, 2013.

[36] S. V. Costa, P. Pingel, S. Janietz, and A. F. Nogueira, "Inverted organic solar cells using nanocellulose as substrate," *Journal of Applied Polymer Science*, vol. 133, no. 28, pp. 6–11, 2016.

[37] Y. Zhou, T. M. Khan, J. C. Liu et al., "Efficient recyclable organic solar cells on cellulose nanocrystal substrates with a conducting polymer top electrode deposited by film-transfer lamination," *Organic Electronics*, vol. 15, no. 3, pp. 661–666, 2014.

[38] M. Nogi, M. Karakawa, N. Komoda, H. Yagyu, and T. T. Nge, "Transparent conductive nanofiber paper for foldable solar cells," *Scientific Reports*, vol. 5, article 17254, pp. 1–7, 2015.

[39] M.-H. Jung, N.-M. Park, and S.-Y. Lee, "Color tunable nanopaper solar cells using hybrid $CH_3NH_3PbI_{3-x}Br_x$ perovskite," *Solar Energy*, vol. 139, pp. 458–466, 2016.

[40] A. Dufresne, "Nanocellulose: a new ageless bionanomaterial," *Materials Today*, vol. 16, no. 6, pp. 220–227, 2013.

[41] D.-Y. Kim, Y. Nishiyama, and S. Kuga, "Surface acetylation of bacterial cellulose," *Cellulose*, vol. 9, no. 3–4, pp. 361–367, 2002.

[42] M. Fumagalli, F. Sanchez, S. M. Boisseau, and L. Heux, "Gas-phase esterification of cellulose nanocrystal aerogels for colloidal dispersion in apolar solvents," *Soft Matter*, vol. 9, pp. 11309–11317, 2013.

[43] M. Fumagalli, D. Ouhab, S. M. Boisseau, and L. Heux, "Versatile gas-phase reactions for surface to bulk esterification of cellulose microfibrils aerogels," *Biomacromolecules*, vol. 14, pp. 3246–3255, 2013.

[44] A. G. Cunha, Q. Zhou, P. T. Larsson, and L. A. Berglund, "Topochemical acetylation of cellulose nanopaper structures for biocomposites: mechanisms for reduced water vapour sorption," *Cellulose*, vol. 21, no. 4, pp. 2773–2787, 2014.

[45] A. Operamolla, S. Casalini, D. Console et al., "Tailoring water stability of cellulose nanopaper by surface functionalization," *Soft Matter*, vol. 14, no. 36, pp. 7390–7400, 2018.

[46] E. D. Glowacki, R. R. Tangorra, H. Coskun et al., "Bioconjugation of hydrogen-bonded organic semiconductors with functional proteins," *Journal of Materials Chemistry C*, vol. 3, pp. 6554–6564, 2015.

[47] S. Chen, Y. Song, and F. Xu, "Highly transparent and hazy cellulose nanopaper simultaneously with a self-cleaning superhydrophobic surface," *ACS Sustainable Chemistry & Engineering*, vol. 6, no. 4, pp. 5173–5181, 2018.

[48] H. Zhu, B. B. Narakathu, Z. Fang et al., "A gravure printed antenna on shape-stable transparent nanopaper," *Nanoscale*, vol. 6, pp. 9110–9115, 2014.

[49] Y. Su, Y. Zhao, H. Zhang, X. Feng, L. Shi, and J. Fang, "Polydopamine functionalized transparent conductive cellulose nanopaper with long-term durability," *Journal of Materials Chemistry C*, vol. 5, no. 3, pp. 573–581, 2017.

[50] M. Österberg, J. Vartiainen, J. Lucenius et al., "A fast method to produce strong NFC films as a platform for barrier and functional materials," *ACS Applied Materials & Interfaces*, vol. 5, no. 11, pp. 4640–4647, 2013.

[51] K. S. Kontturi, K. Biegaj, A. Mautner et al., "Noncovalent surface modification of cellulose nanopapers by adsorption of polymers from aprotic solvents," *Langmuir*, vol. 33, no. 23, pp. 5707–5712, 2017.